Extraction and prediction of Monsoon Intraseasonal Oscillations: An approach based on nonlinear Laplacian spectral analysis

Ajaya Mohan Ravindran and C.T. Sabeerali
Center for Prototype Climate Modelling, New York University Abu Dhabi

Dimitris Giannakis and Andrew J Majda
Center for Prototype Climate Modelling, New York University Abu Dhabi
Department of Mathematics and Center for Atmosphere and Ocean sciences,
Courant Institute for Mathematical Sciences, New York University

Future directions of Subseasonal to Seasonal Prediction over South Asia
29-31 March 2021, IITM

CPCM

جامعة نيويورك ابوظبي
NYU ABU DHABI

Current Status of Extended Range Prediction (ERP) of MISOs

- Various agencies (e.g. IITM/IMD) makes ERP of MISOs. Acknowledging Dr Sahai's seminal contribution here.
- IITM use a coupled model (NCEP CFSv2) outputs to make these predictions
- Extended EOF (EEOF) is used to make these real-time monitoring and ERP
- ERP is carried out on various parameters like rainfall, winds etc.

Can we improve the skill of these predictions?

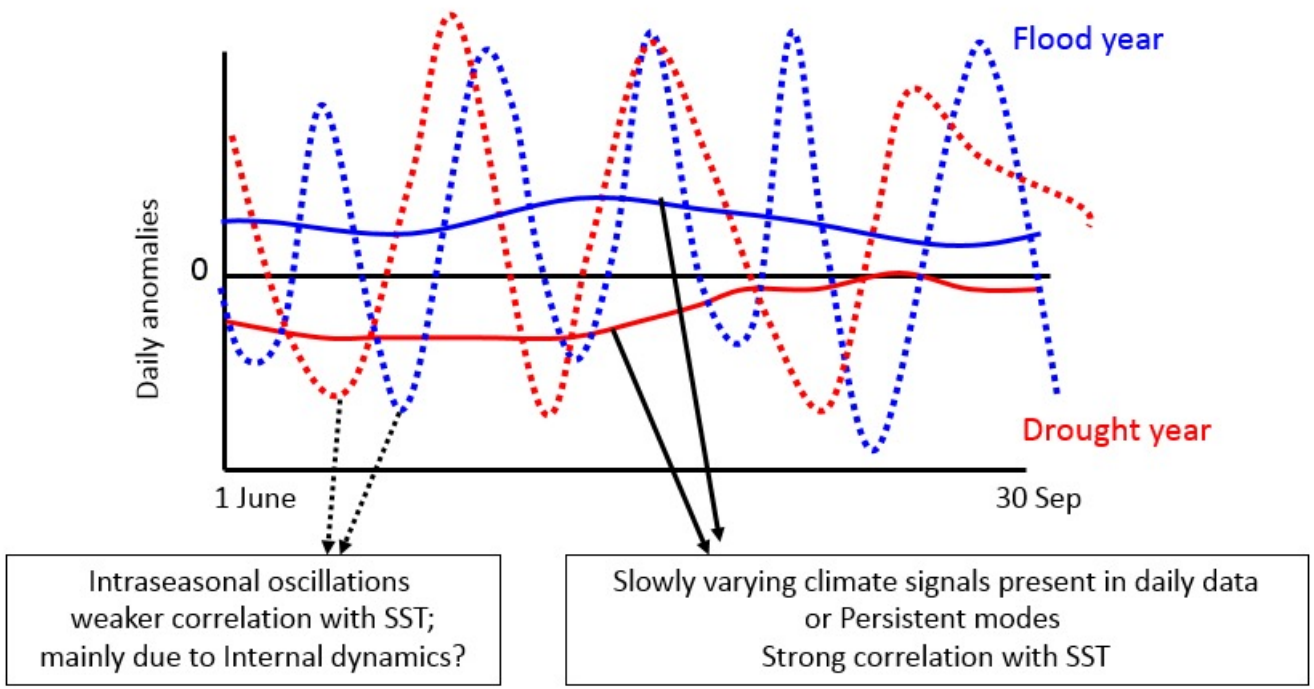

CPCM

جامعة نيويورك ابوظبي
NYU ABU DHABI

Can we improve the skill of these predictions?

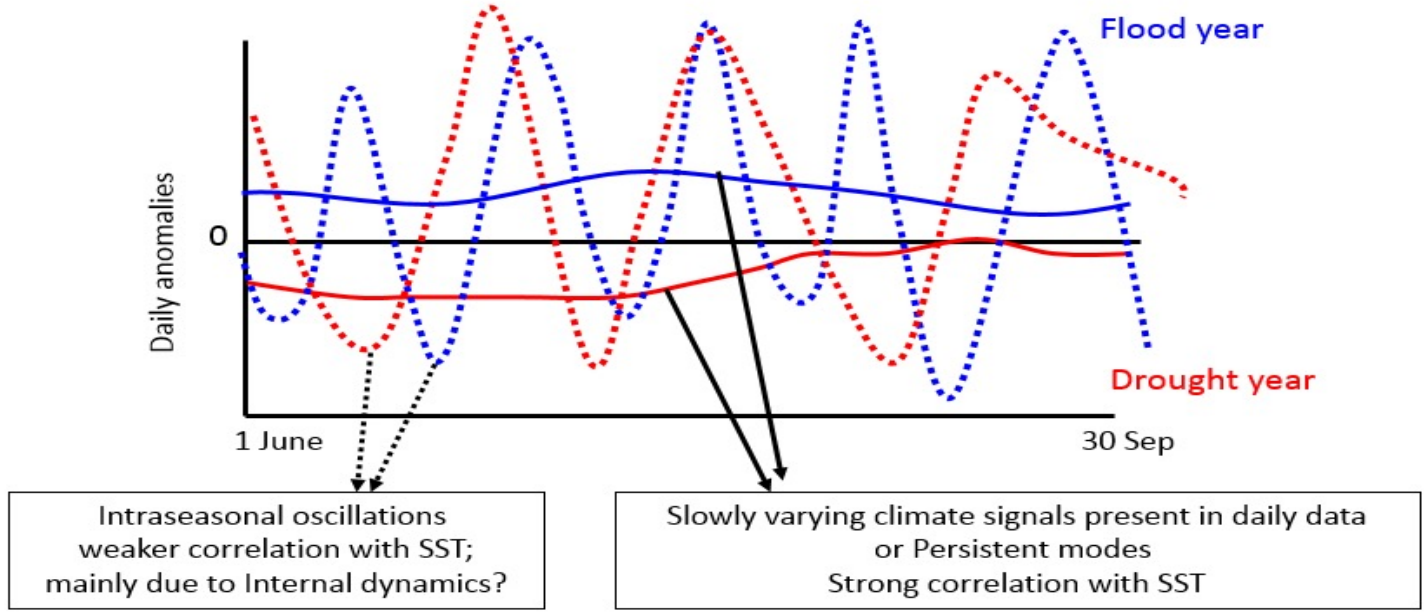

We attempted to devise two methods to address this problem.

1. An alternate method instead of EEOF which is currently used, namely NLSA

2. Predicting NLSA based MISO indices using a physics-constrained low-order stochastic model.

Details Here:

- Sabeerali, Ajayamohan, Giannakis, Majda (Clm Dyn, 2017, 3031-3050)
- Chen, Majda, Sabeerali, Ajayamohan (Jl. Climate, 2018, 4403-4427)

CPCM

جامعة نيويورك ابوظبي
NYU ABU DHABI

Extraction and prediction of indices for monsoon intraseasonal oscillations: An approach based on nonlinear Laplacian spectral analysis (NLSA)

Objectives

•An improved index for the real time monitoring and forecast verification of MISO is developed using nonlinear Laplacian spectral analysis (NLSA) algorithms, which has the potential to capture the low-frequency variability and intermittency.

•Key advantage of NLSA over classical covariance based approach is that it is able to extract modes spanning multiple time scales without requiring adhoc preprocessing (e.g. seasonal partitioning or bandpass filtering etc) of input data

Overview of NLSA

NLSA is a nonlinear data analysis technique that combine ideas from delayed embedding of dynamical systems and kernel methods for harmonic analysis and machine learning to extract spatiotemporal modes of variability from high dimensional time series.

These modes are computed using the Eigen functions of a discrete Laplace-Beltrami operator---- an operator which can be thought of as a local analog of the temporal covariance matrix employed in EOF and EEOF technique, but adapted to the nonlinear geometry of data generated by complex dynamical systems.

Giannakis and Majda, PNAS, 2012

CPCM

جامعة نيويورك ابوظبي
NYU ABU DHABI

NLSA Papers

- Giannakis D, Majda AJ (2012a) Comparing low-frequency and intermittent variability in comprehensive climate model through nonlinear Laplacian spectral analysis. Geophys Res Lett 39:L10710. doi:10.1029/2012GL051575
- Giannakis D, Majda AJ (2012b) Nonlinear Laplacian spectral analysis for time series with intermittency and low-frequency variability. Proc Natl Acad Sci USA 109:2222–2227. doi:10.1073/ pnas.1118984109
- Székely E, Giannakis D, Majda AJ (2016a) Extraction and predictability of coherent intraseasonal signals in infrared brightness temperature data. Clim Dyn 46(5):1473–1502
- Székely E, Giannakis D, Majda AJ (2016b) Initiation and termination of intraseasonal oscillations in nonlinear Laplacian spectral analysis indices. Math Clim Weath Forecast 2(1):1–25. doi:10.1515/ mcwf-2016-0001
- Ww Tung, Giannakis D, Majda AJ (2014) Symmetric and antisymmetric signals in MJO deep convection. Part I: basic modes in infrared brightness temperature. J Atmos Sci 71:3302–3326. doi:10.1175/jas-d-13-0122.1
- Ww Tung, Giannakis D, Majda AJ (2014) Symmetric and antisymmetric signals in MJO deep convection. Part II: Kinematics and thermodynamics, J. Atmos. Sci.
- R. Alexander, Z. Zhao, E. Szekely and D. Giannakis, 2017: Kernel analog forecasting of tropical intraseasonal oscillations, Journal of Atmospheric Sciences, doi:10.1175/JAS-D-16-0147.1

NLSA methodology

We applied NLSA on daily GPCP rainfall data (without performing any pre-filtering or seasonal partitioning) for the period 1997-2014.

Using the GPCP rainfall data $\{x(t_1), \ldots, x(t_s)\}$, NLSA compute a hierarchy of Laplace-Beltrami eigen functions $\phi_0(t_i), \phi_1(t_i), \ldots, \phi_l(t_i)$ which are temporal patterns, that can be thought of as a nonlinear analogs of the PCs in EEOF analysis

Also compute a corresponding collection of spatiotemporal patterns,

$\{x^{(0)}(t_i), x^{(1)}(t_i), \ldots, x^{(l)}(t_i)\}$ such that $\sum_{k=0}^{l} x^{(k)}(t_i)$ approximate the input signal $x(t_i)$

Overview of NLSA algorithms

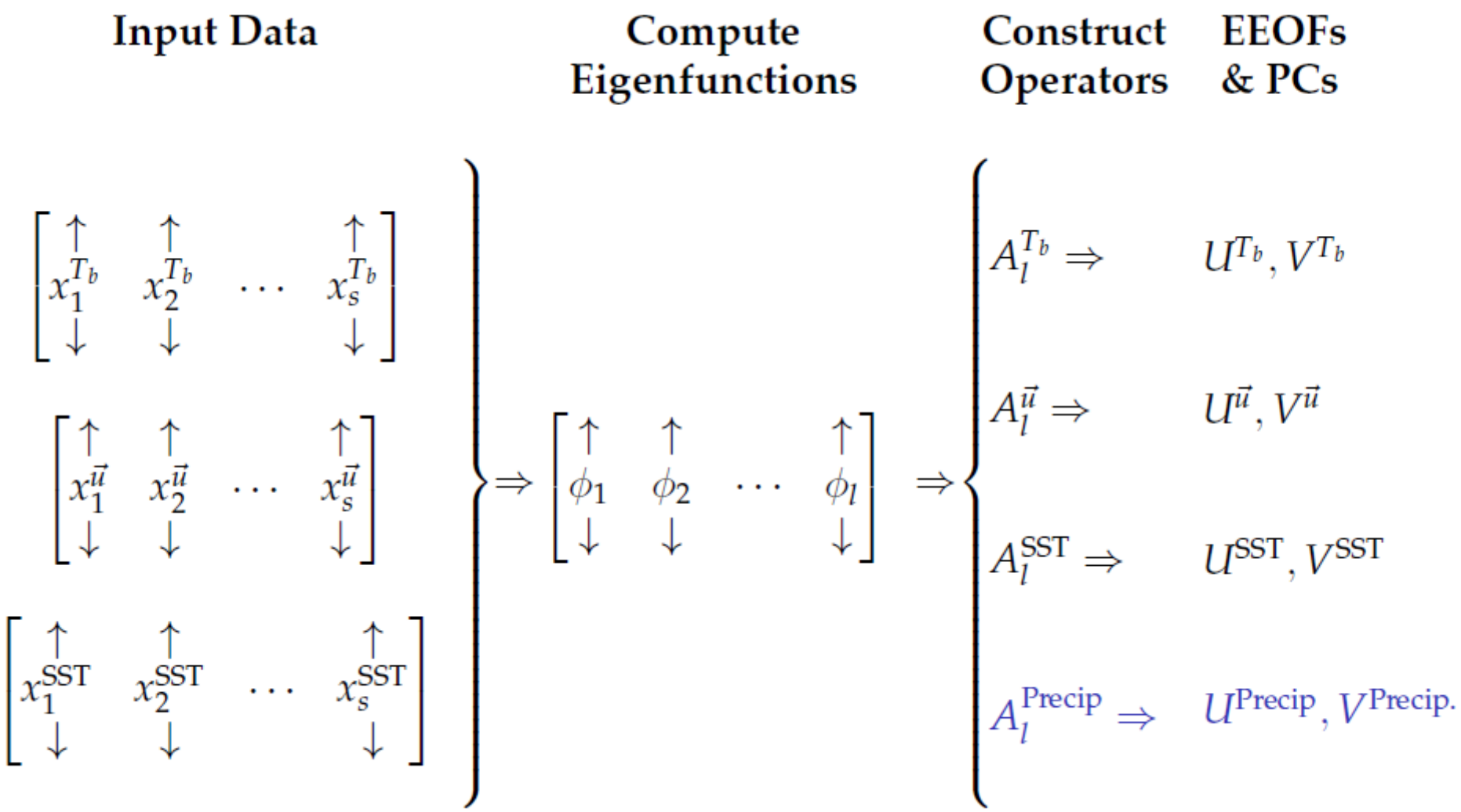

CPCM

جامعة نيويورك ابوظبي
NYU ABU DHABI

Overview of NLSA algorithms

NLSA pipeline consist of three main steps:

1) First step, which is common with EEOF analysis, is to construct a higher dimensional, time-lag embedded datasets

Each snapshot $x(t_i)$ with $i \geq q$ is mapped to the lagged sequence

$$X(t_i) = (x(t_i), x(t_{i-1}), \ldots, x(t_{i-q+1})).$$

After time lagged embedding we have n-q+1 samples for analysis. Where q=number of lags (here we used q= 64 days it is a nominal choice for ISO) and n=physical dimension of GPCP precipitation. We verified our result with different q values, for examples q=34 and 48 and 90 days. q=90 days are in good agreement with our nominal choice q=64 days. Smaller q values exhibit mixing of different timescales.

2. Next step is to compute the Kernal matrix K with entries (similar to covariance matrix in EEOF)

$$K(X(t_i), X(t_j)) = \exp\left(-\frac{\|X(t_i) - X(t_j)\|^2}{\epsilon \xi(t_i)\xi(t_j)}\right).$$

Here ϵ is a positive kernel band width parameter and $\xi(t_i)$ are phase space velocities measuring local time tendency of data through

$$\xi(t_i) = \|X(t_i) - X(t_{i-1})\|.$$

We used $\epsilon = 2\ \epsilon$ in the interval 2-5 does not make qualitative changes in results

Overview of NLSA algorithms

Kernal values $K(X(t_i), X(t_j))$ provide a nonlinear measure of similarity between samples $X(t_i)$ and $X(t_j)$ with

$K(X(t_i), X(t_j))$ =1 meaning $X(t_i)$ and $X(t_j)$ are highly similar

= 0 meaning highly dissimilar

3) After computing the Kernal matrix K, normalizing it to get Markov matrix P using a normalization procedure.

- Conceptually, these eigen functions as nonlinear anologs of Principle components in EEOF analysis. Used to create spatiotemporal reconstructions and phase composites.
- A key advantage of NLSA over standard covariance based methods (like EOF) is that by design requires no adhoc preprocessing of data (detrending, temporal filtering etc).

CPCM

Sabeerali, Ajayamohan, Giannakis, Majda (Clm Dyn, 2017)

جامعة نيويورك ابوظبي

NYU ABU DHABI

Hierarchy of spatiotemporal modes revealed by NLSA

• Leading six LB Eigen functions whose time series and power spectral densities functions. Blue lines: 1/(90 days) and 1/(30 days) frequencies. Red Lines: 95% confidence intervals based on Markov red noise spectrum.

Periodic modes

• Modes 1 and 2 represent the annual cycle.

• Modes 3 and 4 represent semiannual variability.

MISO modes

• Modes 5 & 6 together represent the full life cycle of MISO. Spectral peaks in the 1/(30 days) - 1/(60 days) frequency band. Confirmed by spatial structures. Exhibit strong seasonality.

2003

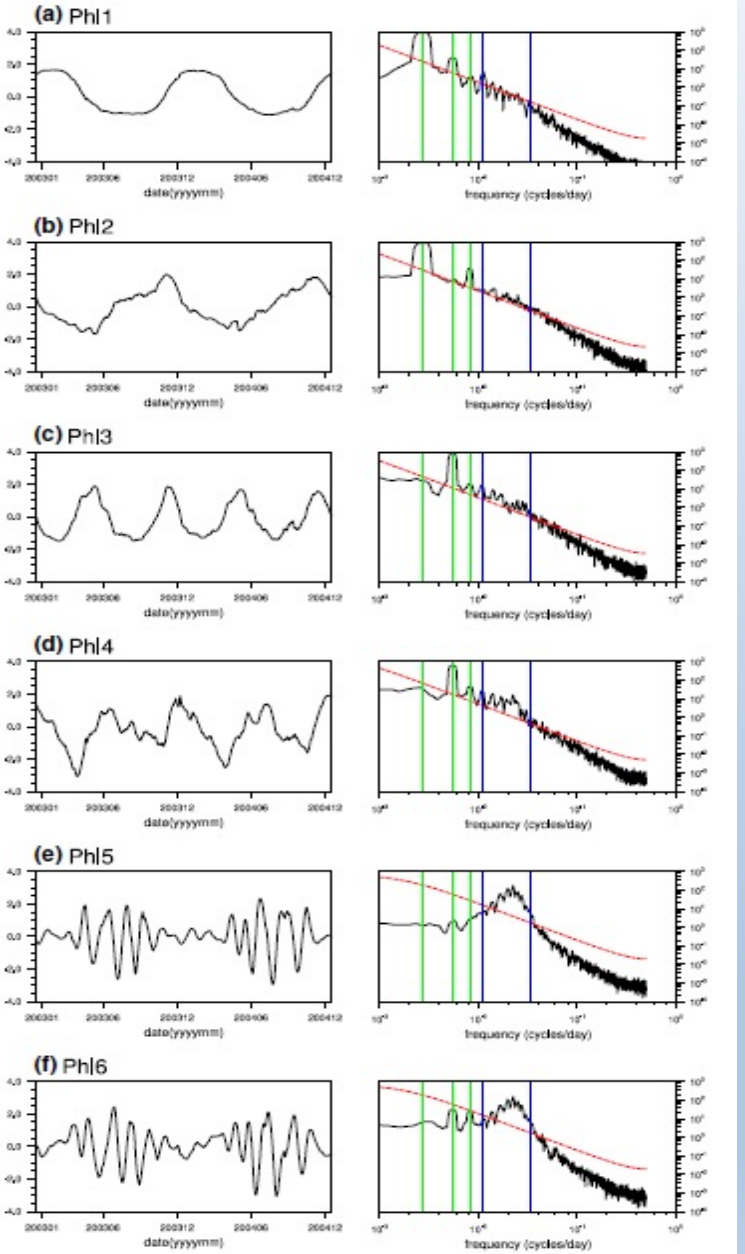

Sabeerali, Ajayamohan, Giannakis, Majda (Clm Dyn, 2017)

CPCM

جامعة نيويورك ابوظبي
NYU ABU DHABI

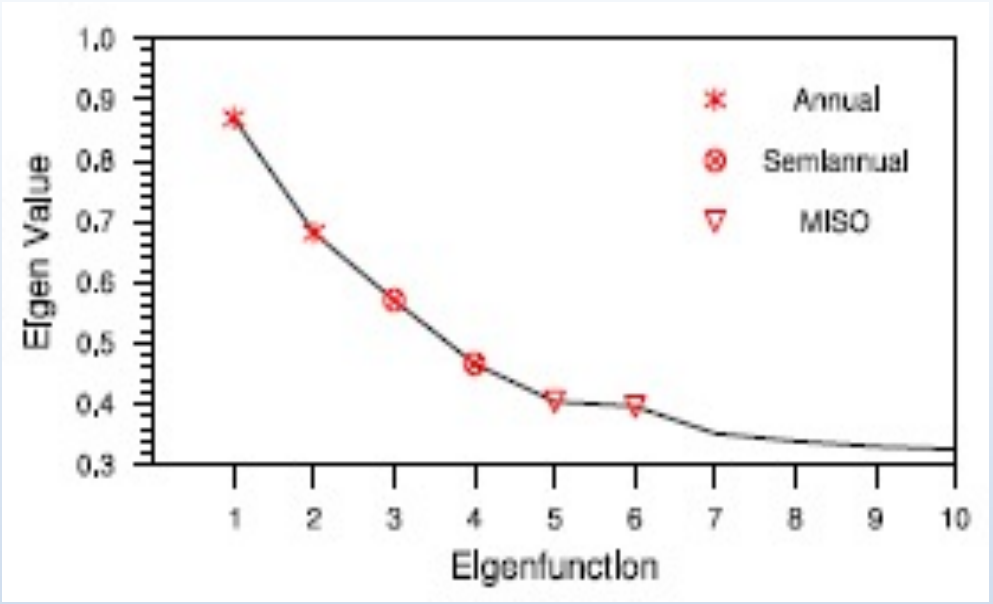

Eigenvalues corresponding to the leading 10 Laplace-Beltrami eigen functions.

Laplace Beltrami eigen functions corresponding to MISO

Detailed view also illustrate the absence of high frequency noise from these two time series.

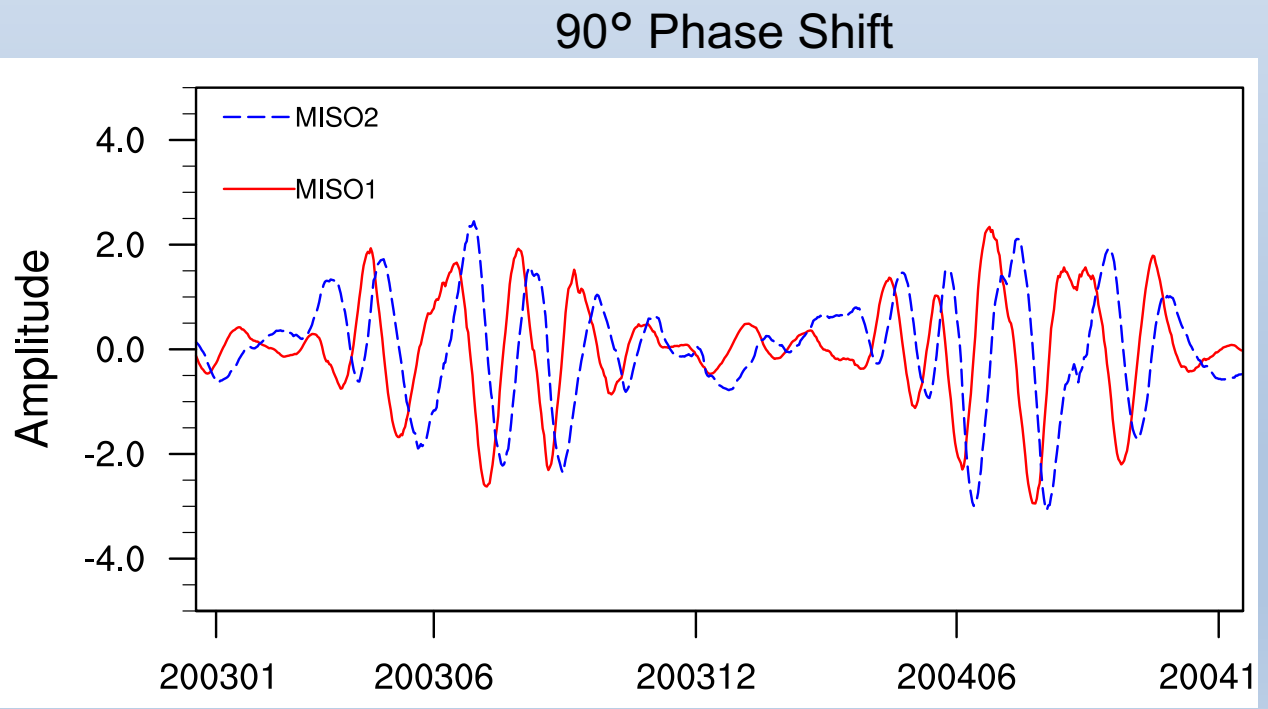

PDFs of NLSA & EEOF MISO modes

NLSA

EEOF-MISO indices are more Gaussian than NLSA

EEOF

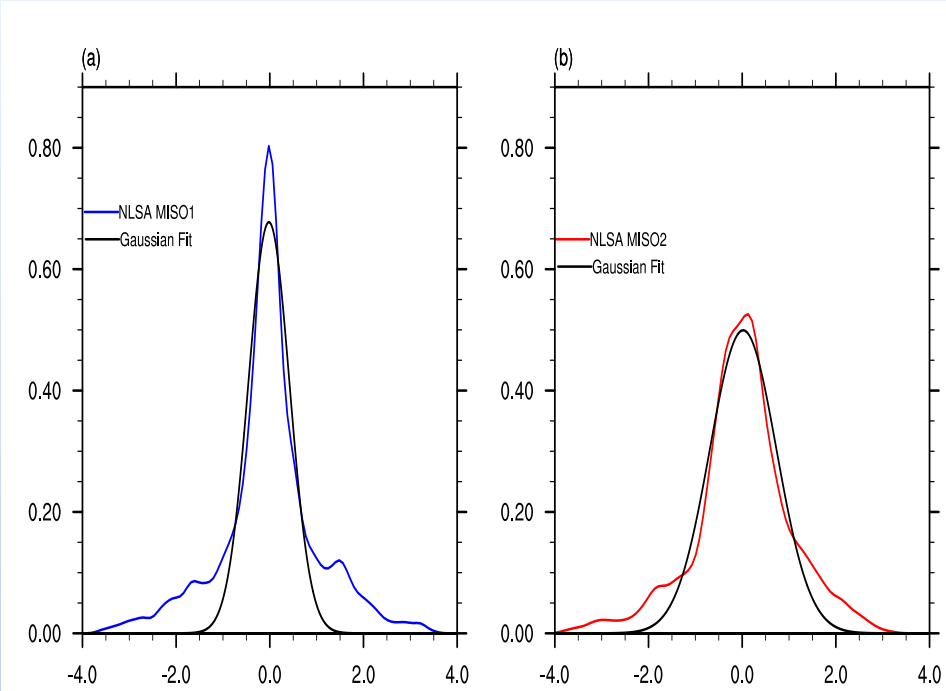

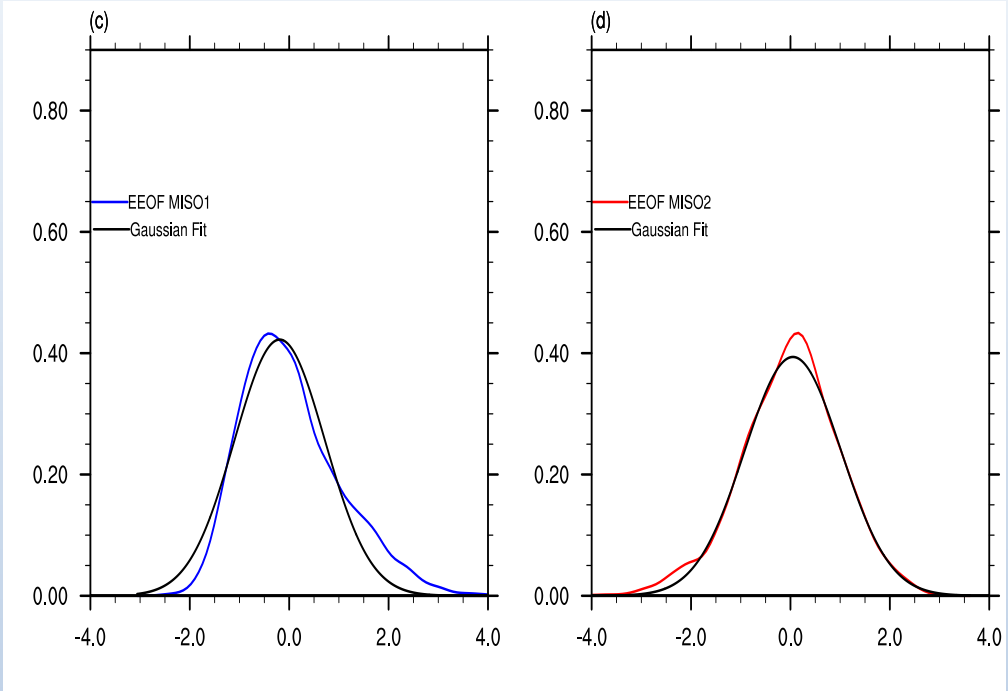

Black curves represent Gaussian fits estimated via nonlinear least squares.

PDFs of these modes have fat tails when computed from the year round data, and their kurtosis values (k=7.6 and 3.8) are significantly higher (leptokurtic) than the k=3 kurtosis of the Gaussian. This non-Gaussian fat-tailed PDFs is consequence of intermittency.

This non-Gaussianity of the NLSA MISO modes contribute to their higher discriminating power compared to classical linear approaches.

CPCM

Sabeerali, Ajayamohan, Giannakis, Majda (Clm Dyn, 2017)

جامعة نيويورك ابوظبي

NYU ABU DHABI

Temporal evolution of JJAS MISO indices & Amplitude

Red: NLSA and Blue: EEOF

•NLSA and EEOF time series are in moderately good qualitative agreement, although the temporal evolution of NLSA modes is markedly more coherent.

• MISO events detected via NLSA tend to be more persistent.

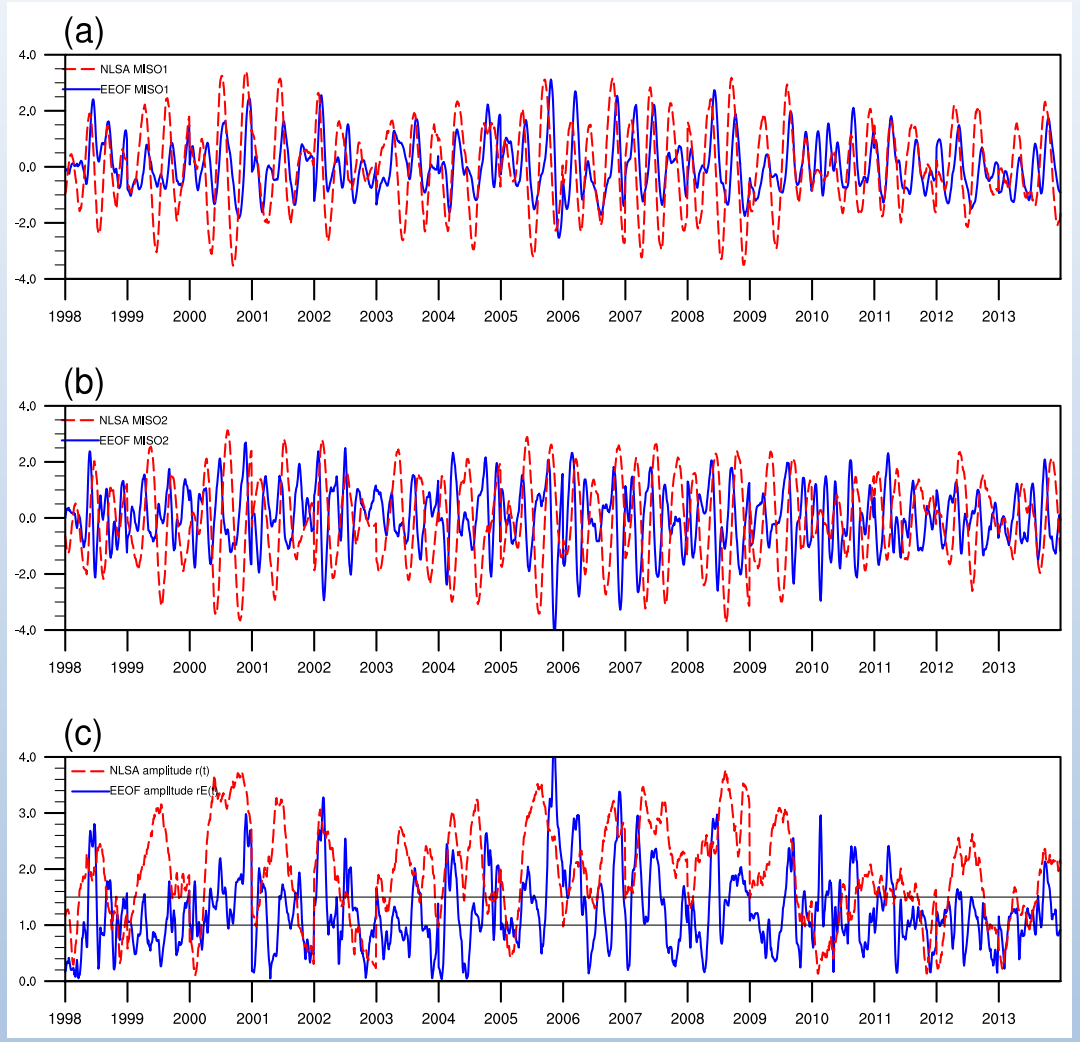

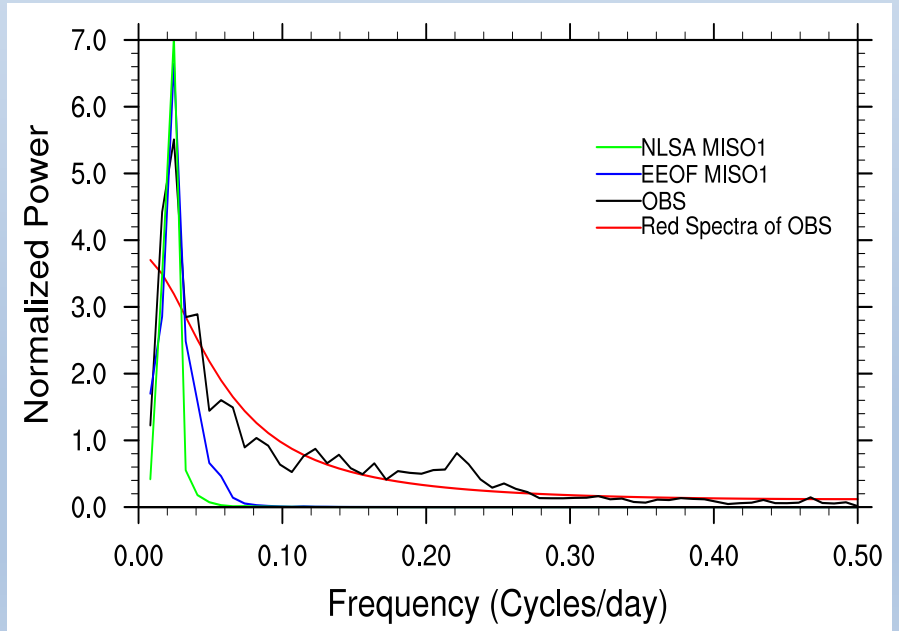

In general spectra of NLSA have smaller high frequency power than the EEOF spectra.

Sabeerali, Ajayamohan, Giannakis, Majda (Clm Dyn, 2017)

CPCM

جامعة نيويورك ابوظبي
NYU ABU DHABI

Spatial reconstructed pattern of MISO

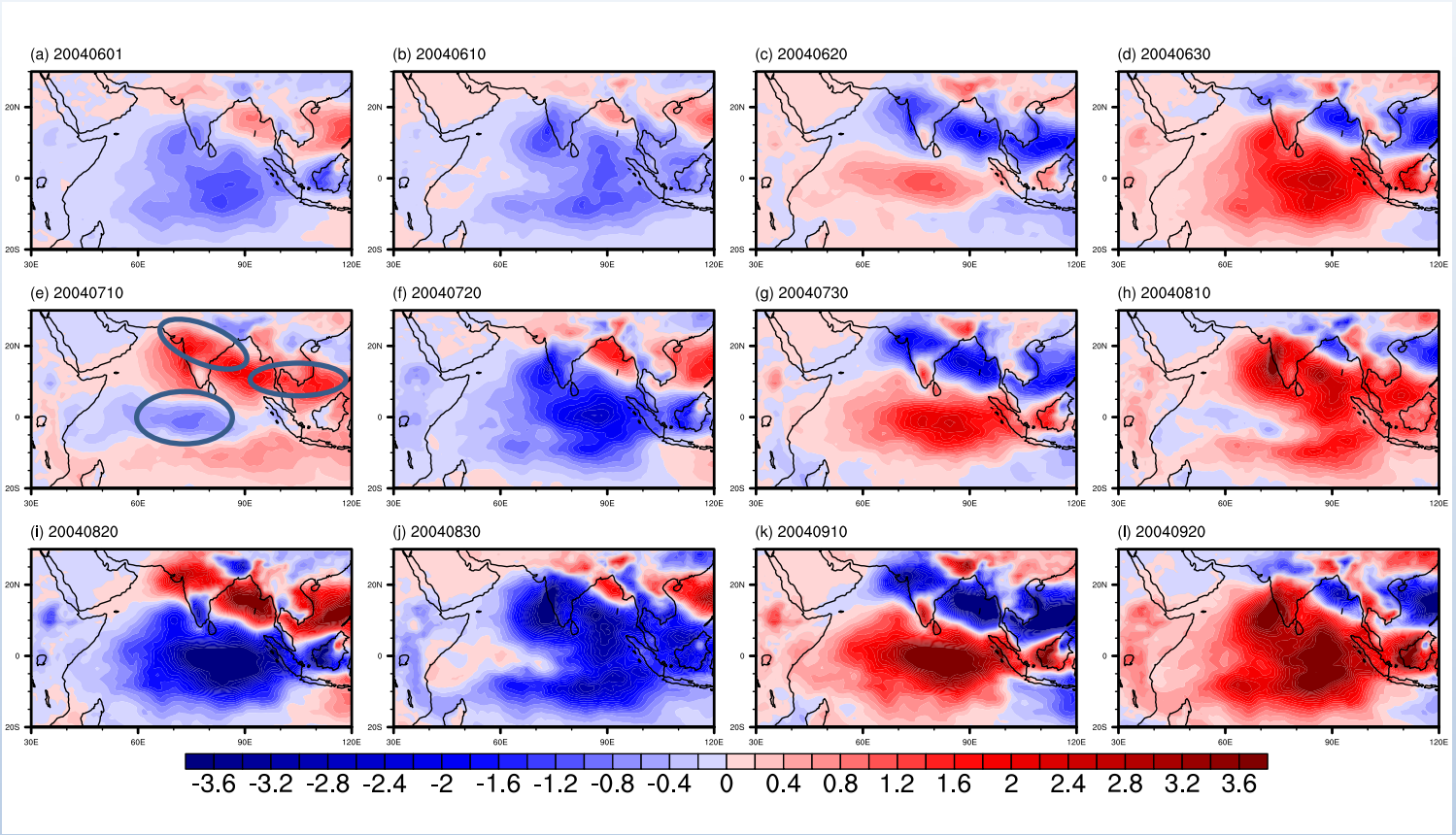

Spatial reconstruction of the 2004 monsoon

Note regional heat sources

In the spatial domain, NLSA MISO modes display the characteristic pattern of northeastward propagating anomalies associated with the MISO.

Sabeerali, Ajayamohan, Giannakis, Majda (Clm Dyn, 2017)

CPCM

جامعة نيويورك ابوظبي
NYU ABU DHABI

Composite Spatial Structure obtained from NLSA/EEOF MISO modes

OLR and 850 wind **Precipitation and 850 wind**

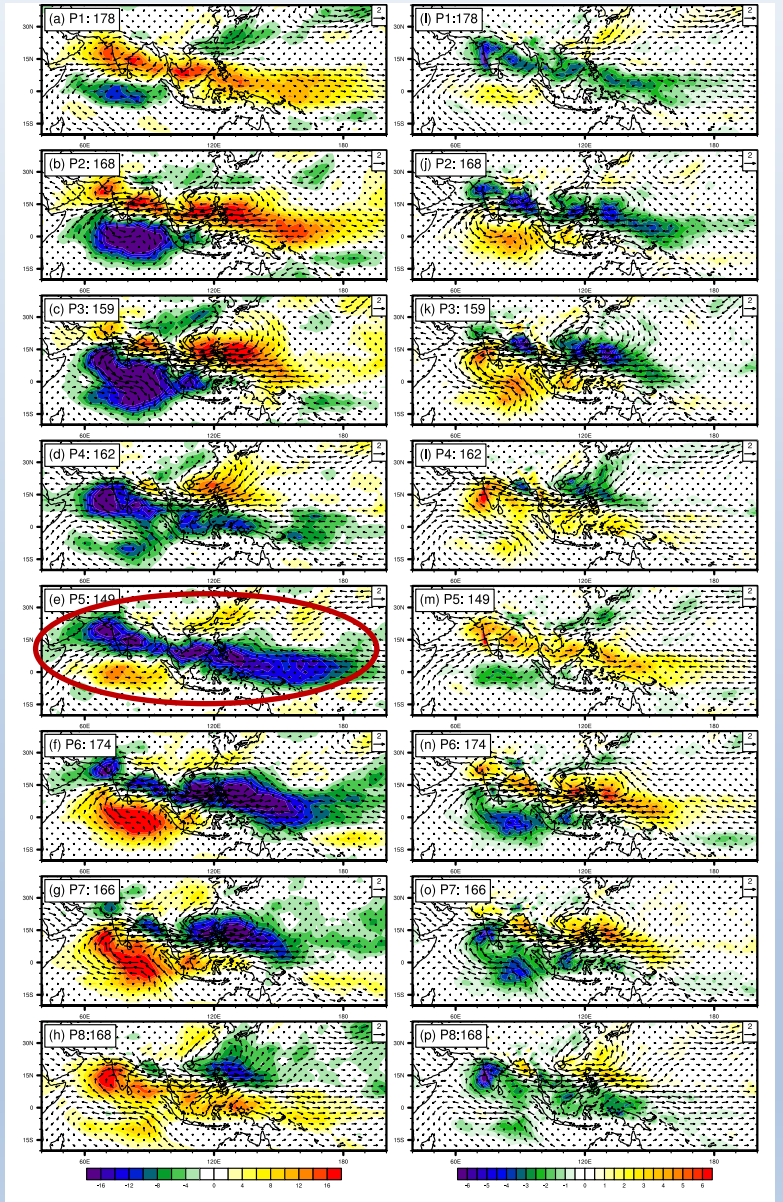

Init alies
ove

Subseq ıdian
subcont

Qua ptured
witl Pacific
is st

Propaga
subcont

Brea

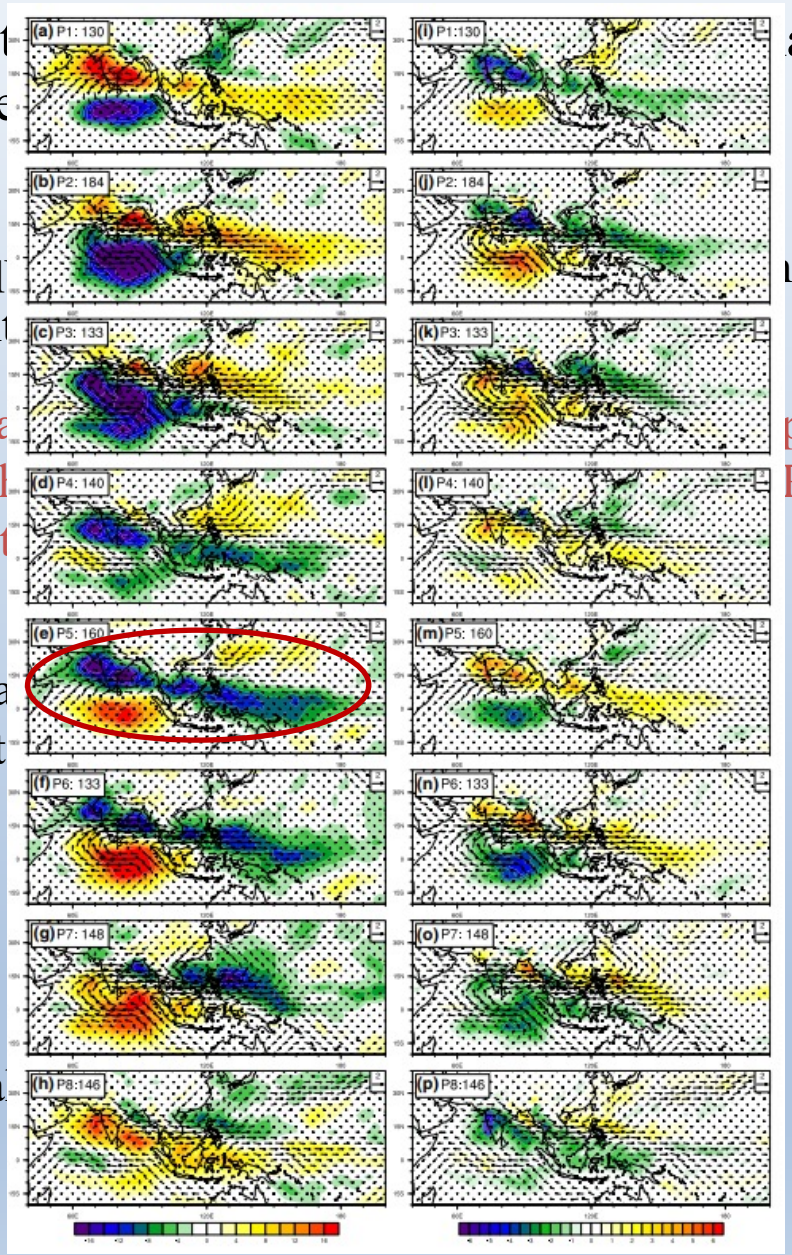

CPCM

Sabeerali, Ajayamohan, Giannakis, Majda (Clm Dyn, 2017)

جامعة نيويورك ابوظبي
NYU ABU DHABI

Percentage of fractional variance of band-pass filtered rainfall anomalies explained by the spatial composite from NLSA and EEOF

- NLSA yields a realistic variance pattern and captures the regional centers of MISO activity.
- Compared to EEOF-based variance map, NLSA explains larger fractional variance over regional heat sources including the western Pacific, Western Ghats, the adjoining Arabian Sea.

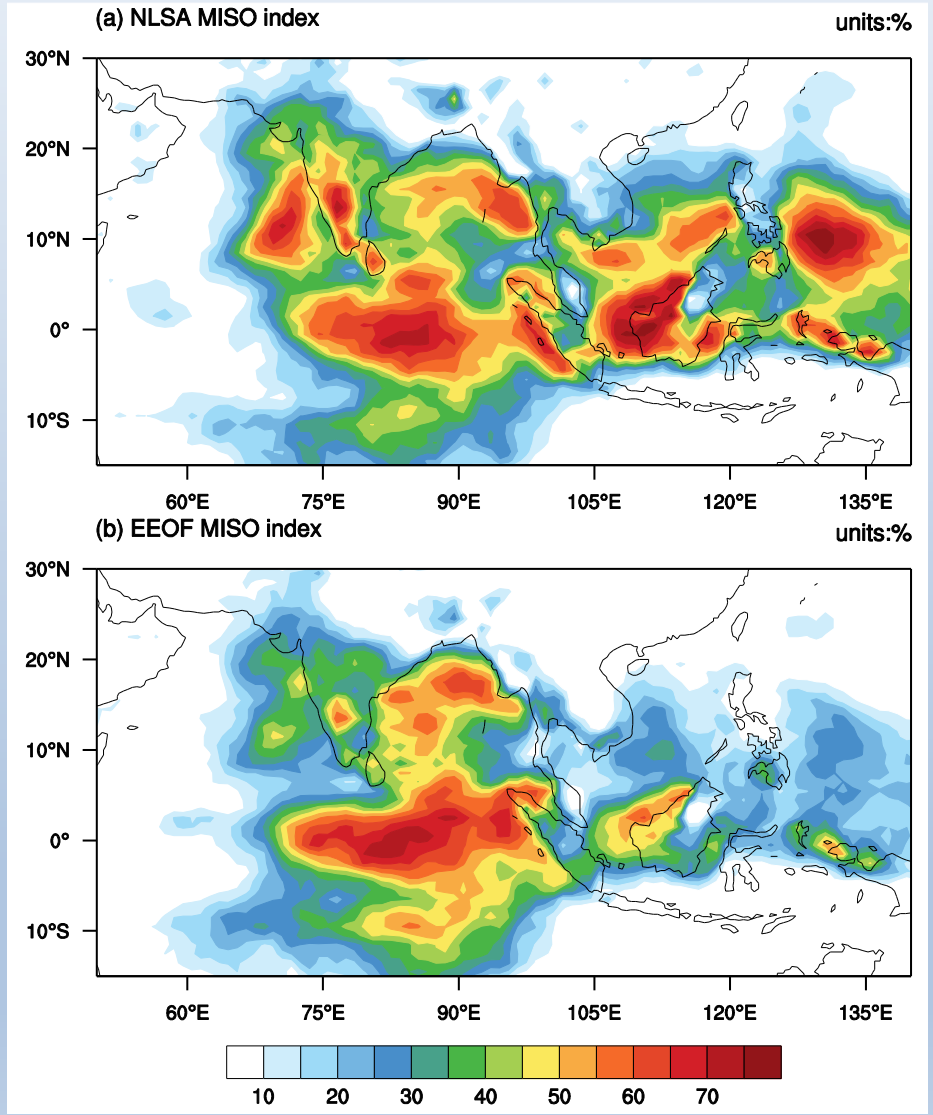

Sabeerali, Ajayamohan, Giannakis, Majda (Clm Dyn, 2017)

CPCM

جامعة نيويورك ابوظبي
NYU ABU DHABI

NLSA and EEOF MISO indices in terms of temporal correlation structure

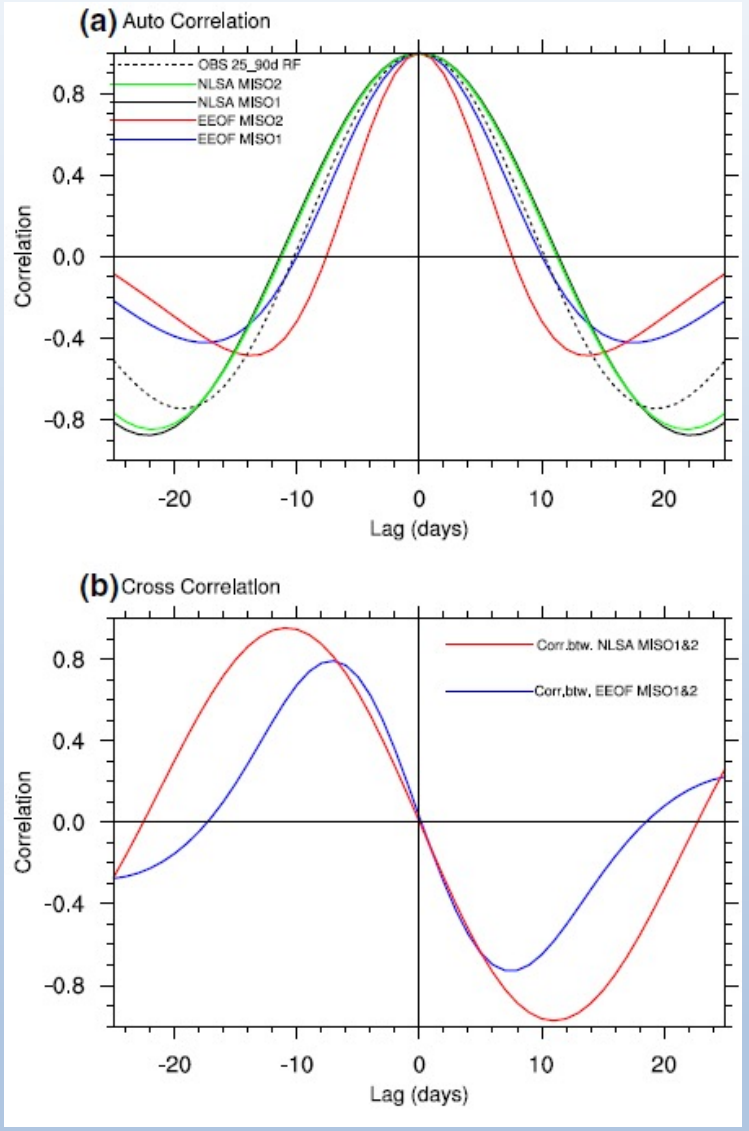

(a) Autocorrelation of NLSA and EEOF MISO indices compared with the autocorrelation of band-pass filtered rainfall anomalies over monsoon core region.

In general auto-correlation of NLSA modes are closer to observations than the EEOF modes, especially at longer lags.

(b) Cross-correlation functions of NLSA and EEOF MISO modes

Cross-correlation between NLSA MISO modes, which are uncorrelated at lag zero by orthogonality of eigen functions. Exhibit a near-sinusoidal behavior with a reemergence of correlation at 11 days lags. Indicative of a coherent, and hence predictable, harmonic oscillator.

In case of EEOF modes, cross cross-correlation is characterized by marked amplitude decay, with minima/maxima occurring earlier and attaining smaller absolute values.

NLSA retain their memory for a longer period, while capturing the dominant spectral peak of MISO efficiently.

CPCM

جامعة نيويورك ابوظبي
NYU ABU DHABI

Does this technique work on real-time monitoring of MISO indices?

We use precipitation field from 45 days operational integrations of NCEP CFSv2 (obtained from IITM; Sahai et al. 2013; Abhilash et al. 2014) to create hindcast of the NLSA MISO1 and MISO2 indices and demonstrate the skill of these hindcasts by comparing the predicted values of the indices against true value computed from GPCP

In each monsoon season, 25 simulations with different initial conditions were performed starting from May 31 to September 28 at 5 days intervals and each initial condition runs involve 40 ensemble members

We use the out-of-sample extension technique to compute the predicted MISO indices from CFSv2

Forecast skill of NLSA MISO indices

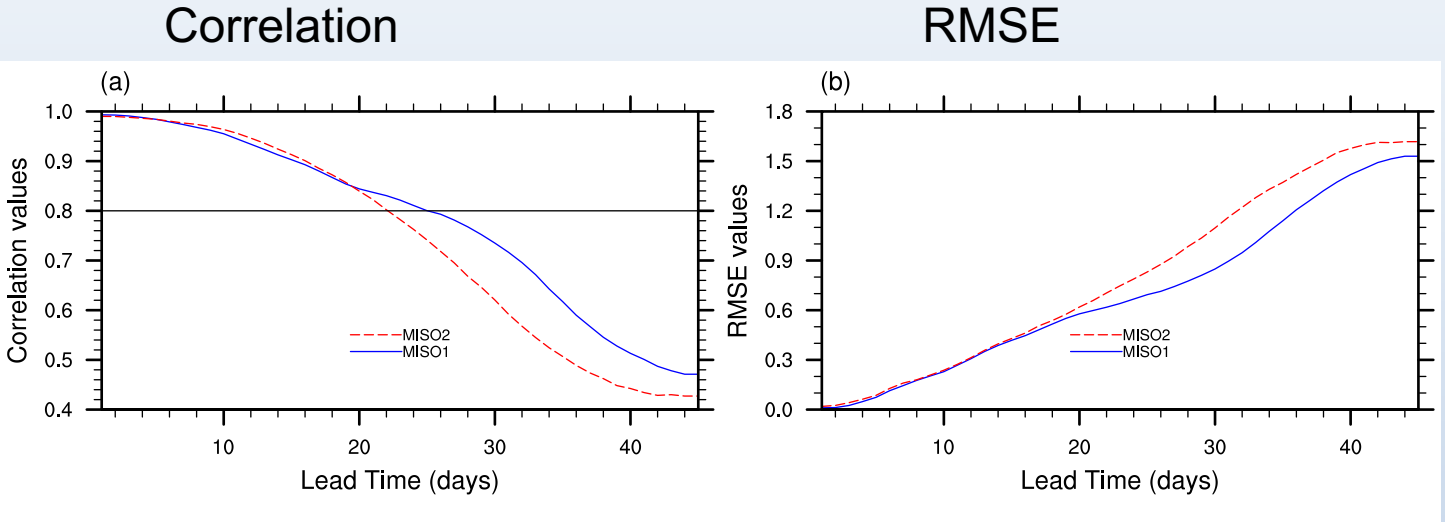

- PC score for both MISO1 and MISO2 exhibit an initial period of persistence to >0.9 values for up to ~ 10 days leads
- PC scores then begin a rapid decay, but remain greater then 0.8 for ~ 3 weeks.
- RMSE scores show a nearly linear increase with lead time, crossing the 1 SD threshold after ~3 weeks.
- NLSA MISO indices remain predictable out to ~ 3 weeks.

CPCM

Sabeerali, Ajayamohan, Giannakis, Majda (Clm Dyn, 2017)

جامعة نيويورك ابوظبي
NYU ABU DHABI

Evolution of NLSA MISO indices from CFSv2 and GPCP rainfall

- In the first case predicted trajectory successfully tracks the truth for up to 32 days, and then slightly deviate from the truth.
- In the second case, predicted trajectory realistically captures truth for up to 16 days and then deviate from the truth.
- In the last two bottom panels, prediction is reasonably good up to ~ 10 days and then failed to track the truth.
- Out of 75 test cases analyzed, 78% are comparably successful to the cases in top two panels and 22% are comparably unsuccessful as the cases in bottom two panels.
- Forecast skill can have large spread depending on the initial data.
- On an average the forecast of the NLSA MISO indices generated using CFSv2 runs are useful out to ~3 weeks lead time.

Top two panels: Successful cases
Bottom two panels: Failed cases

GPCP CFSv2

Successful cases

Failed cases

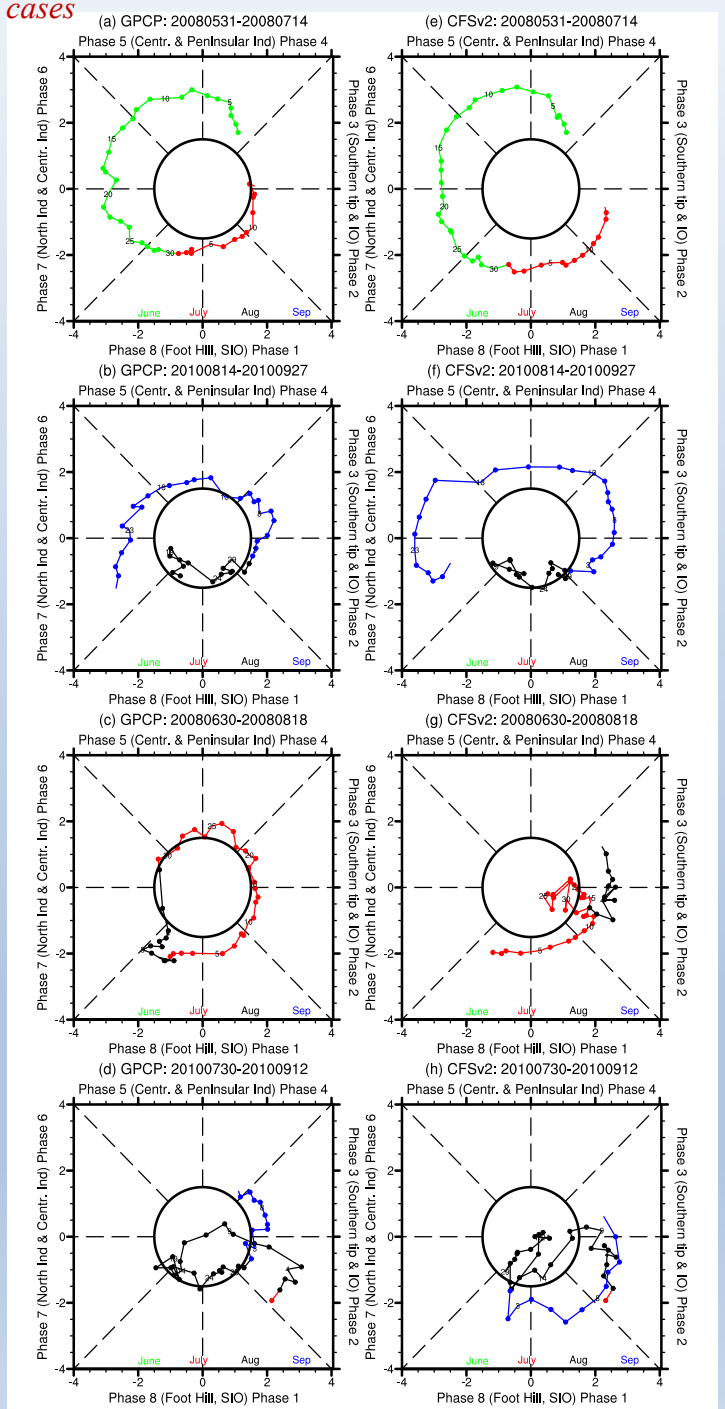

Sabeerali, Ajayamohan, Giannakis, Majda (Clm Dyn, 2017)

CPCM

Conclusions

- An improved index for real-time monitoring and forecast verification of monsoon intraseasonal oscillation (MISO) is introduced using NLSA algorithms.
- Using NLSA a hierarchy of Lapalce-Beltarmi (LB) Eigen functions are extracted from unfiltered daily rainfall data from GPCP over the south Asian summer monsoon domain.
- Two modes representing the full lifecycle of MISO are identified from the LB Eigen functions.
- These modes have number advantages over MISO modes extracted from EEOF analysis including higher memory and predictability, stronger amplitude and higher fractional explained variance over the western Pacific, Western Ghats and adjoining Arabian Sea regions, and more realistic representation of the regional heat sources over the Indian and Pacific Oceans.
- Real time prediction of NLSA-derived MISO indices is demonstrated via extended-range hindcasts based on NCEP CFSv2 45 days operational output. It is shown that in these hindcasts the NLSA MISO indices remain predictable out to ~ 3 weeks.

Acknowledgments: NYUAD RI Funds, NMM Grant, ONR MURI Grant

C. T. Sabeerali. R. S. Ajayamohan, D. Giannakis, and Andrew J. Majda, 2017: Extraction and prediction of indices for monsoon intraseasonal oscillations: an approach based on nonlinear Laplacian spectral analysis, *Climate Dynamics*., doi: 10.1007/s00382-016-3491-y

CPCM

جامعة نيويورك ابوظبي
NYU ABU DHABI

Paying homage to Andy (passed away on March 12, 2021)

Andrew Majda

Principal Investigator

Andrew Majda is a Professor of Mathematics at the Courant Institute of Mathematical Sciences in New York. His research interests center around stochastic statistical behavior of turbulent dynamical systems in climate atmosphere ocean science. He blends math theory, qualitative and quantitative models, designs numerical algorithms, and combines with physical reasoning to gain new insight into extremely complex systems. Professor Majda received his Ph.D. in Mathematics from Stanford University.

THE CENTER FOR
PROTOTYPE CLIMATE MODELING

CPCM

جامعة نيويورك ابوظبي
NYU ABU DHABI

Seasonal Mean Rainfall

Summer

A large rainfall zone covers most of south Asia, and equatorial Indian/Pacific Ocean.

Winter

The precipitation zone moves southward over the Indian Ocean. There is no rainfall over south Asia.

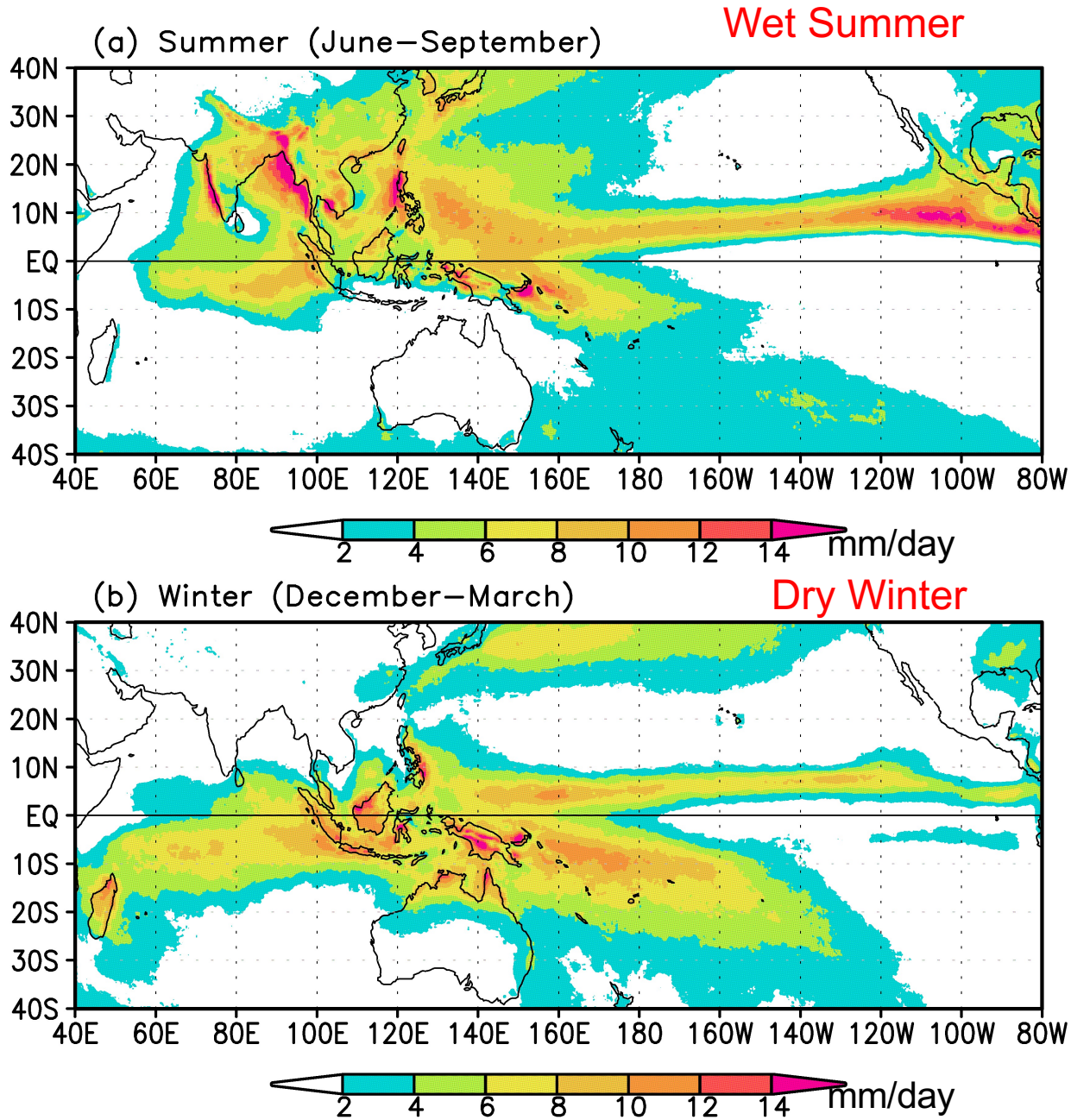

CPCM

جامعة نيويورك ابوظبي
NYU ABU DHABI

Intraseasonal Variability of Indian Monsoon

Monsoon Intraseasonal Oscillations

Note the variability of Monsoon Intraseasonal Oscillations (MISOs)

- Aperiodic nature of MISOs
- Timing and amplitude of rainfall during active/ break phases
- In spite of initial good spells of rainfall, 1986 turned out to be a drought
- Our task here is to predict the onset, amplitude, residence time and spatial structure of these of these oscillations at least 3 weeks in advance (Extended Range Prediction).
- Very important for various planning purposes. For instance, farmers can decide on sowing dates

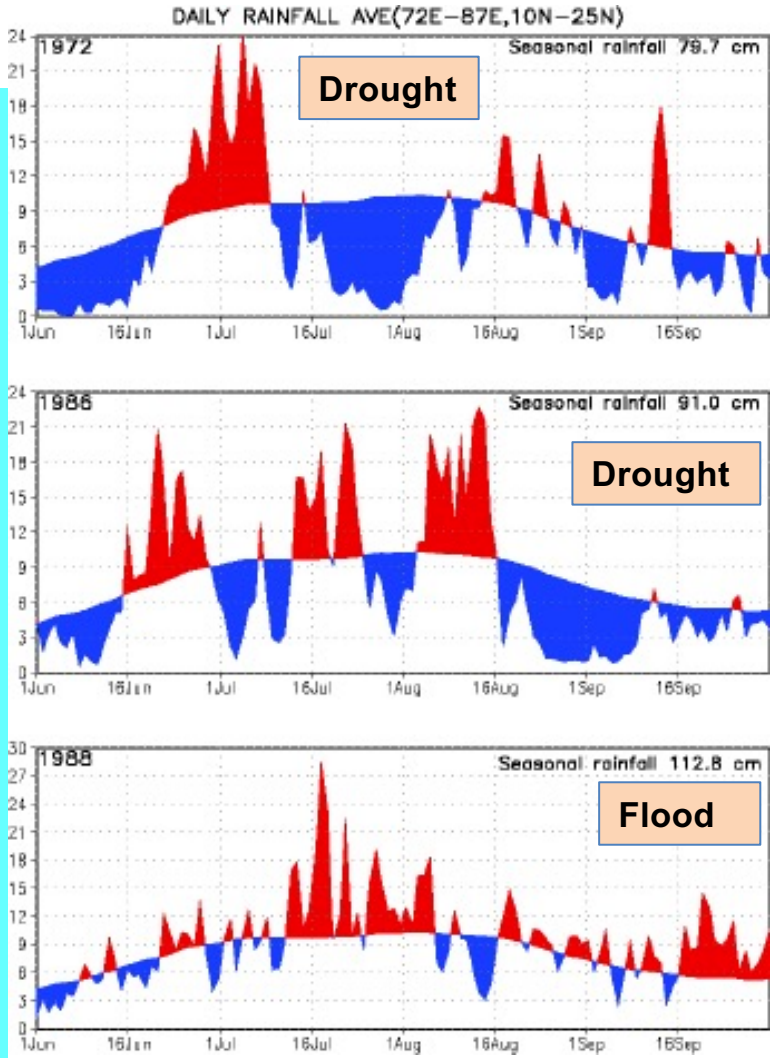

Daily rainfall anomalies on daily climatological mean over the monsoon trough region

CPCM

جامعة نيويورك ابوظبي
NYU ABU DHABI

Overview of NLSA algorithms

Kernal values $K(X(t_i), X(t_j))$ provide a nonlinear measure of similarity between samples $X(t_i)$ and $X(t_j)$ with

$K(X(t_i), X(t_j))$ =1 meaning $X(t_i)$ and $X(t_j)$ are highly similar
=0 meaning highly dissimilar

K has size SxS where S=s-q. Due to exponential decay of the kernel, the entries of K below a given threshold can be set to zero leading to a sparse matrix. Here we set largest 650 nonzero entries in each row of K (which corresponds to ~ 10% of total number of samples

3) After computing the Kernal matrix K, normalizing it to get Markov matrix P using following normalization procedure.

$$q_i = \sum_{j=1}^{S} K_{ij}, \quad K'_{ij} = \frac{K_{ij}}{q_i q_j}, \quad d_i = \sum_{j=1}^{S} K'_{ij}, \quad P_{ij} = \frac{K_{ij}}{d_i}, \qquad (1)$$

NLSA temporal patterns are then computed by the eigen vectors of the Laplacian matrix L=I-P $L\phi_k = \lambda_k \phi_k, \quad \phi_k = (\phi_{1k}, \phi_{2k}, \ldots, \phi_{Sk})^\top,$

Spatiotemporal Reconstruction

With the predicted MISO indices in hand, the final step is to recover the spatiotemporal MISO pattern in physical space. This require combination of time series and spatial bases.

Let z_i be an d-dimensional vector of gridded precipitation values over ASM domain at time *i.* Here *i* is an integer ranging from 1 to n,

First construct a time lagged datasets utilizing Taken delay of embedding. q denotes embedding window size.

Lagged embedding matrix can be written as

$$X = \begin{pmatrix} z_1 & z_2 & \cdots & z_{n-2q+1} \\ z_2 & z_3 & \cdots & z_{n-2q+2} \\ \vdots & \vdots & \ddots & \vdots \\ z_{q-1} & z_q & \cdots & z_{n-q-1} \\ z_q & z_{q+1} & \cdots & z_{n-q} \end{pmatrix} = \begin{pmatrix} z_1 & z_2 & \cdots & z_{N-q+1} & z_{N-q+2} & \cdots & z_{N-1} & \boxed{z_N} \\ z_2 & z_3 & \cdots & z_{N-q+2} & z_{N-q+3} & \cdots & \boxed{z_N} & z_{N+1} \\ \vdots & \vdots & \ddots & \vdots & \cdots & \cdots & \cdots & \vdots \\ z_{q-1} & z_q & \cdots & z_{N-1} & \boxed{z_N} & \cdots & z_{N+q-3} & z_{N+q-2} \\ z_q & z_{q+1} & \cdots & \boxed{z_N} & z_{N+1} & \cdots & z_{N+q-2} & z_{N+q-1} \end{pmatrix},$$

N=n-2q+1 here q is actually dq but d is omitted for simplicity

CPCM

Chen, Majda, Sabeerali, Ajayamohan (2017, submitted in *J. Climate*)

جامعة نيويورك ابوظبي
NYU ABU DHABI

Compute Spatial Basis

The relation between spatiotemporal reconstruction X, the time series Φ and the spatial basis

A is simply given by $X = A\Phi^T$,

$$A = \frac{1}{\|\Phi\|^2} X\Phi = \frac{1}{\|\Phi\|^2} \begin{pmatrix} X_1 & \cdots & X_N \end{pmatrix} \cdot \begin{pmatrix} \Phi_1 \\ \vdots \\ \Phi_N \end{pmatrix},$$

X is of size qxN and A is of size qx1 and Φ is of size Nx1

A is spatial basis

Compute Spatiotemporal Pattern

Reconstruction is obtained from the following eqn: $X^f = A.\Phi^f$

where X^f and Φ^f are reconstruction of spatiotemporal pattern and eigen function time series

$$A.\Phi^f = \begin{pmatrix} A_1 \\ A_2 \\ \vdots \\ A_q \end{pmatrix} \cdot \left(\Phi_1^f, \quad \Phi_2^f, \quad \cdots, \quad \Phi_q^f \right)$$

$$= \begin{pmatrix} A_1\Phi_1^f & A_1\Phi_2^f & \cdots & \boxed{A_1\Phi_q^f} \\ A_2\Phi_1^f & A_2\Phi_2^f & \cdots & A_2\Phi_q^f \\ \vdots & \vdots & \cdots & \vdots \\ A_{q-1}\Phi_1^f & \boxed{A_{q-1}\Phi_2^f} & \cdots & A_{q-1}\Phi_q^f \\ \boxed{A_q\Phi_1^f} & A_q\Phi_2^f & \cdots & A_q\Phi_q^f \end{pmatrix}$$

Now take the average of diagonal element to get the spatiotemporal pattern of first time unit

Out-of-sample extension

In the real-time prediction, it is important to compute NLSA eigen function for previously unseen samples.

Suppose we have given a lagged sequence of precipitation snapshots,

$Y = (y(t'_i), y(t'_{i-1}), \ldots, y(t'_{i-q+1}))$ where t'_i represent time at forecast verification, $y(t'_j)$ precipitation over the ASM domain as in training data.

Here Y is constructed from CFSv2 output, or a concatenated sequence to CFSv2 and GPCP data (to provide precipitation snapshot at time prior to CFSv2 initialization.

Consider now the eigen function time series $\phi_k(t_i)$ with corresponding eigen value λ_k

Each value can be naturally associated with the training sample in lagged embedding space $\mathbb{R}^N$ i.e we have the mapping $X(t_i) \mapsto \phi_k(t_i)$

In the Nytrom out-of-sample technique, that mapping is extended to arbitrary point $Y \in \mathbb{R}^N$ subjected to a consistency requirement on the training data. i.e $Y \in \mathbb{R}^N$ we compute a quantity $\hat{\phi}_k(Y)$ such that if Y happens to be equal to some X(ti) in the training dataset, then $\hat{\phi}_k(Y) = \phi_k(t_i)$.

CPCM

NYU ABU DHABI

Out-of-sample extension

We first compute the pairwise kernel values between Y and the samples in the training datasets, $\hat{K}_j(Y) = K(Y, X(t_j))$

Then perform diffusion map normalization procedure,

$$\hat{K}_j(Y) = \frac{\hat{K}_j(Y)}{q_j}, \quad \hat{d}(Y) = \sum_{j=1}^{S} \hat{K}'_j(Y), \quad \hat{P}_j(Y) = \frac{K'_j(Y)}{\hat{d}(Y)},$$

Where q_j is determined from (1). Note that

And if Y=X(t_i) then $\sum_{j=1}^{S} P'_j(Y) = 1$ and if Y=X(t_i) then $\hat{P}_j(Y) = P_{ij}$

Introducing the row vector $\hat{P}(Y) = (\hat{P}_1(Y), \ldots, \hat{P}_S(Y))$

Out of sample extension of ϕ_k is then given by,

$$\hat{\phi}_k(Y) = \frac{1}{1-\lambda_k} \hat{P}(Y)\phi_k.$$

Extension become ill conditioned when $1 - \lambda_k \approx 0$

Eigenfunction with large roughness value cannot be robustly extended.

CPCM

جامعة نيويورك ابوظبي
NYU ABU DHABI

NLSA MISO indices

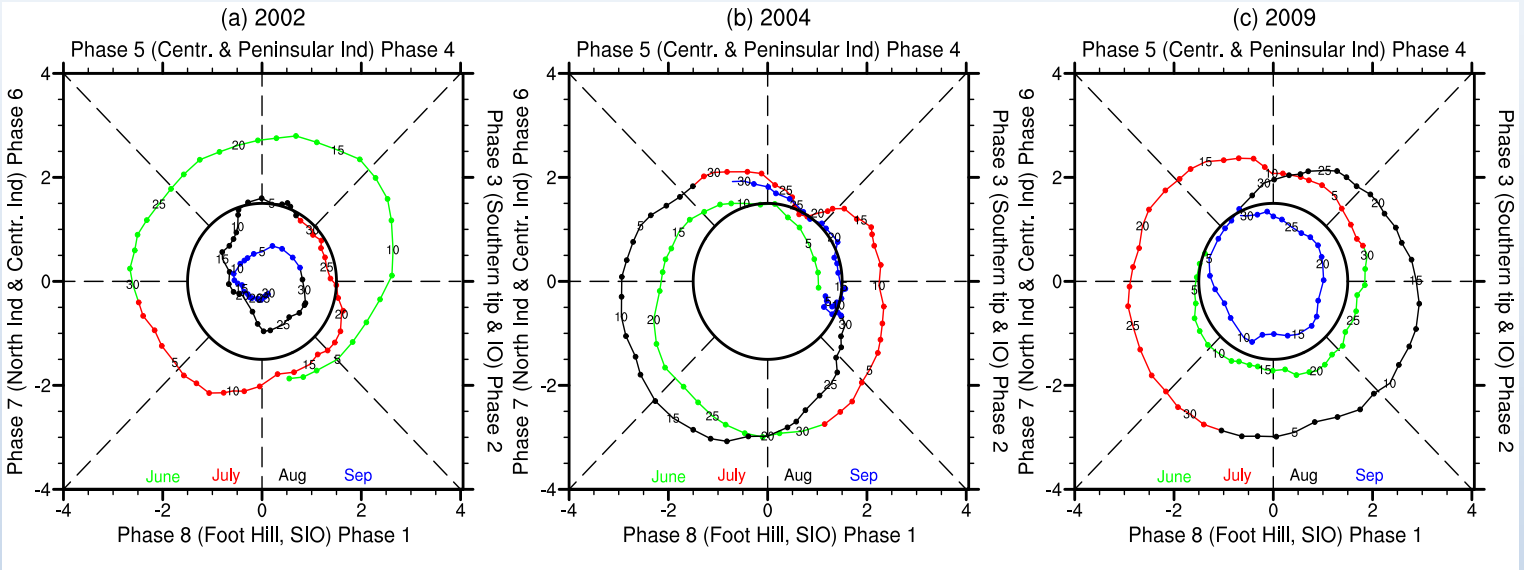

2D phase diagram constructed from the NLSA MISO indices for the three drought years.

- An anticlockwise propagation from the phase 1 represent MISO's northward propagation. The circle centered the origin has radius equal to 1.5 which is our threshold for identifying significant MISO events based on the MISO amplitude index

MISO amplitude at time t is obtained via

$$r(t) = \sqrt{\frac{\mathrm{MISO1}(t)^2}{\sigma_1^2} + \frac{\mathrm{MISO2}(t)^2}{\sigma_2^2}},$$

r(t)=1.5 value is close to the JJAS standard deviation of NLSA MISO indices.

- It is evident that MISO activity does not always begin in phase 1 and end in phase 8; a behavior which has also been observed in the case of the MJO

Sabeerali, Ajayamohan, Giannakis, Majda (Clm Dyn, 2017)

CPCM

جامعة نيويورك ابوظبي
NYU ABU DHABI

Comparison with EEOF based MISO indices

To place our result in context, we compare the NLSA-based MISO modes with EEOF-based modes (Suhas et al. 2013). EEOF based MISO indices are currently used for real-time monitoring of MISO at IITM, and one of the objective our study is to explore ways to improve the skill of the real-time forecasts.

EEOF MISO modes are computed following Suhas et al. (2013). i.e perform EEOF analysis on longitudinally averaged (over 60.5E-95.5E) GPCP rainfall data for JJAS and latitudes 12.5S-30.5N, after removing the climatological mean and first three harmonics of the seasonal cycle. We use 15 EEOF lags sampled once per day.

At a given time we define the MISO indices $MISO1_E(t)$ and $MISO2_E(t)$ from EEOF PCs 1 and 2 and also define EEOF-based MISO amplitude index

$$r_{\mathrm{E}}(t) = \sqrt{\frac{\mathrm{MISO1_E}(t)^2}{\sigma_{1\mathrm{E}}^2} + \frac{\mathrm{MISO2_E}(t)^2}{\sigma_{2\mathrm{E}}^2}}.$$

CPCM

Sabeerali, Ajayamohan, Giannakis, Majda (Clm Dyn, 2017)

جامعة نيويورك ابوظبي
NYU ABU DHABI

Composite Spatial Structure obtained from EEOF MISO modes

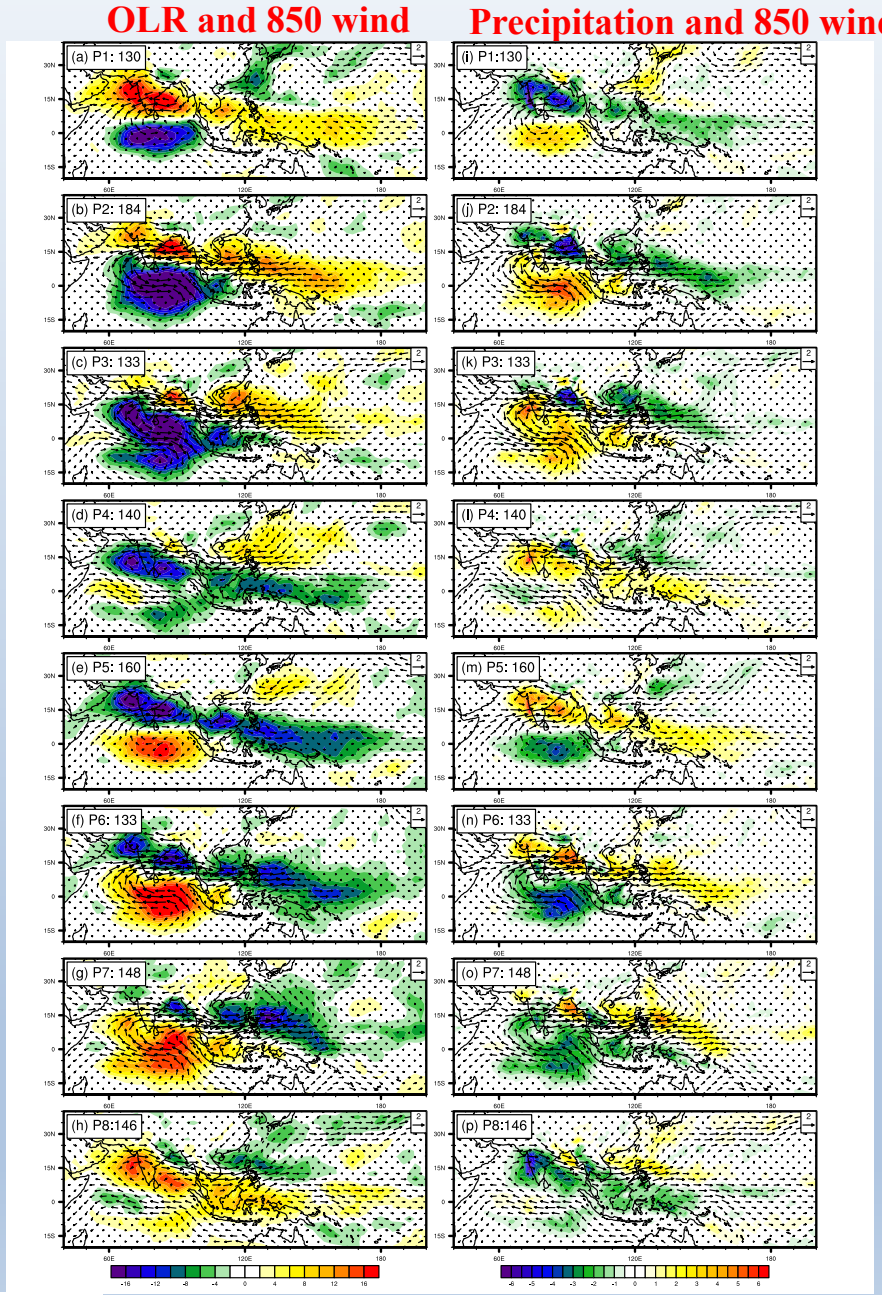

Composites spatial structure clearly exhibit the typical lifecycle of the MISO, including its northeastward propagation and zonal and meridional structure, but certain features are not as well represented as in NLSA.

EEOF based composite have weaker loading of convection anomalies over the Maritime continent and Western Pacific and therefore a less developed tilted zonal convection band beyond the date line.

Sabeerali, Ajayamohan, Giannakis, Majda (Clm Dyn, 2017)

CPCM

جامعة نيويورك ابوظبي
NYU ABU DHABI

- C. T. Sabeerali. R. S. Ajayamohan, D. Giannakis, and Andrew J. Majda, 2017: Extraction and prediction of indices for monsoon intraseasonal oscillations: an approach based on nonlinear Laplacian spectral analysis, *Climate Dynamics*., doi: 10.1007/s00382-016-3491-y, in press

- Nan Chen, Andrew J. Majda, C. T. Sabeerali and R. S. Ajayamohan, 2017: Predicting the Monsoon Intraseasonal Oscillations through a Low-Order Nonlinear Stochastic Model, *Journal of Climate* (under review)

- R. Alexander, Z. Zhao, E. Szekely and D. Giannakis, 2017: Kernel analog forecasting of tropical intraseasonal oscillations, Journal of Atmospheric Sciences, doi:10.1175/JAS-D-16-0147.1, in press

Mean July Rainfall and Surface Convergence

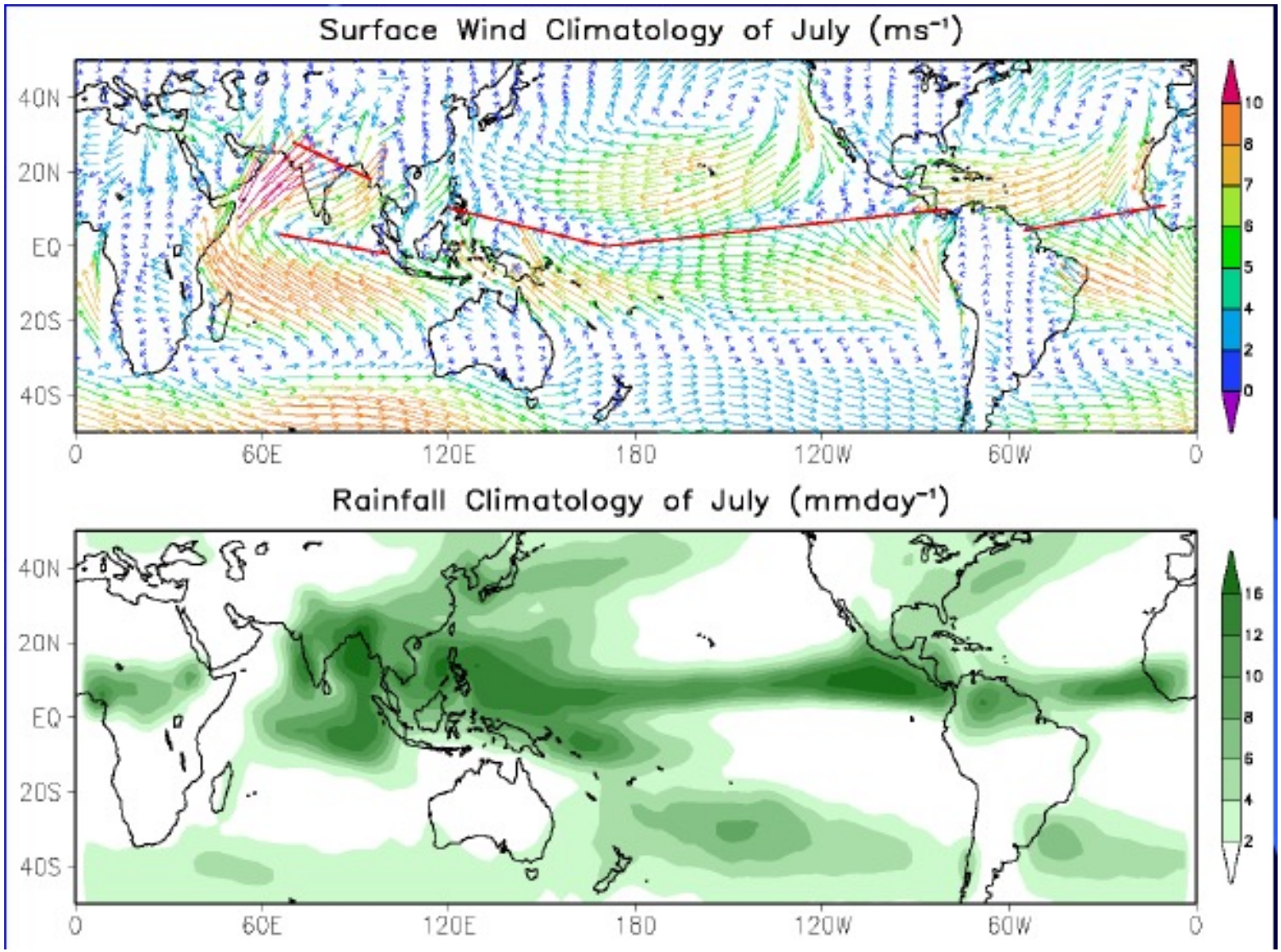

CPCM

جامعة نيويورك ابوظبي
NYU ABU DHABI

Advantage of NLSA over covariance based Linear methods such as EEOF or MSSA

- Improved time scale separation and ability to detect intermittent patterns through the use of kernel methods in conjunction with Time delay embedding
- Covariance based techniques have potential inadequency in capturing the rare/extreme events in complex nonlinear dynamics. NLSA capture the nonlinear and non-Guassian features associated with a time series (here MISO)
- Do not require any preprocessing of data (e.g detrending, spatiotemporal filtering or seasonal partitioning or longitudinal averaging) and capture both intermittency and low frequency variability.
- Use a Laplace-Beltrami operator which is nonlinear analogue of covariance matrix used in linear methods

Power Spectral Densities

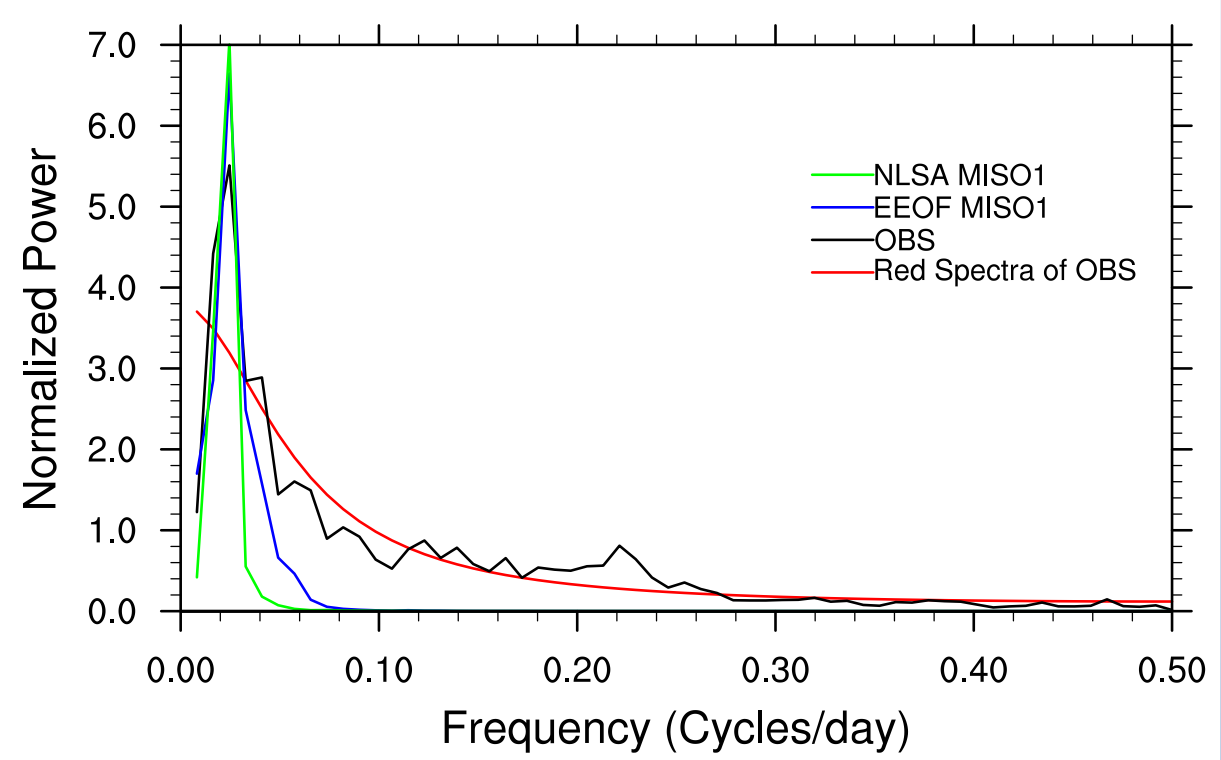

MISO indices obtained through either NLSA or EEOF capture the central peak between 1/(30 days)and 1/(60 days) observed in raw rainfall anomalies, and are also effective in removing the high frequency content present in rainfall data.

In general spectra of NLSA have smaller high frequency power than the EEOF spectra.

NLSA MISO indices vs Actual Rainfall data

Red Line: NLSA MISO2 mode

Black Line: Unfiltered JJAS rainfall anomalies over the central Indian domain (10.5N-25.5N, 70.5E-85.5E)

Blue Line: Band-pass filtered (25-90 days) JJAS rainfall anomalies over the central Indian domain.

- In all the three drought years NLSA index is able to capture the active and break phases associated with the Indian summer monsoon.

- MISO1 also correlate well with the active and break phases, but because this mode has a 90° phase difference with MISO2, the correlation exhibits a time lag (not shown here).

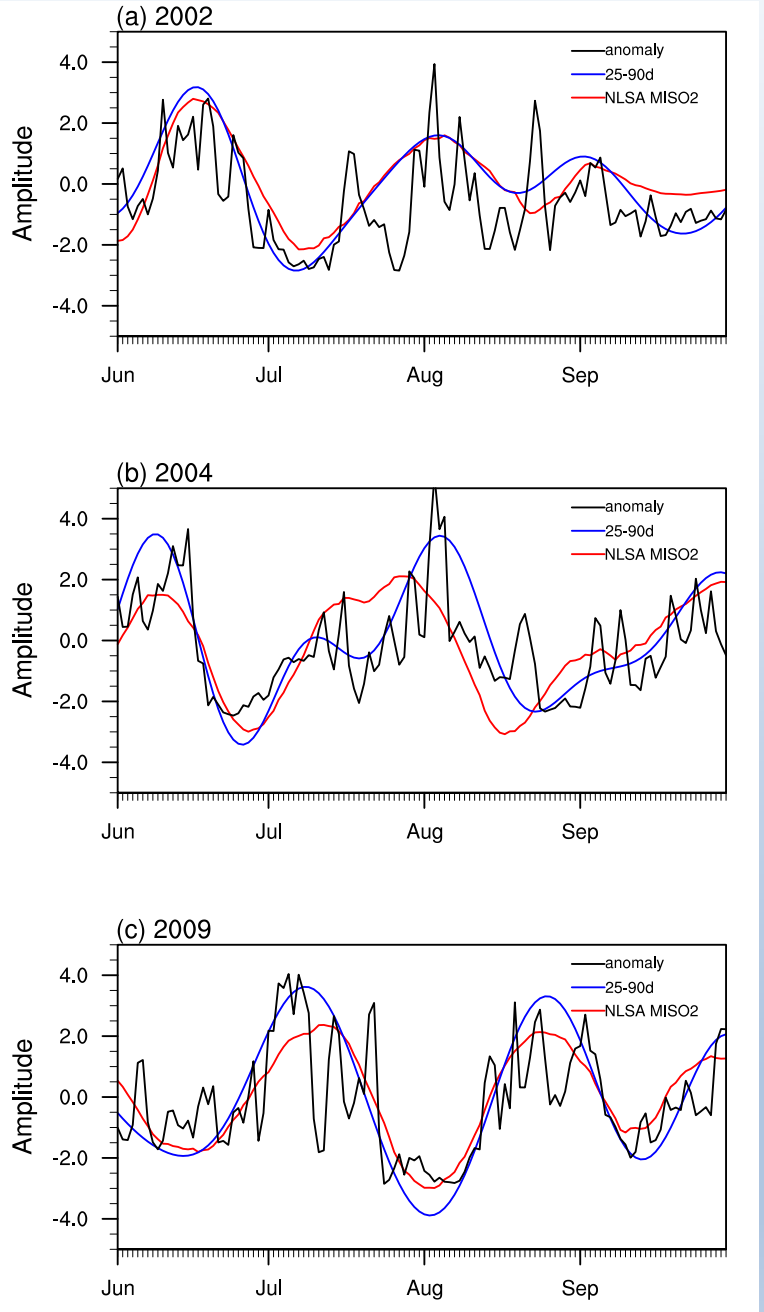

CPCM

Sabeerali, Ajayamohan, Giannakis, Majda (Clm Dyn, 2017)

جامعة نيويورك ابوظبي
NYU ABU DHABI